

Prashant Mandare  
H. Henning Winter

## Ultraslow dynamics in asymmetric block copolymers with nanospherical domains

Received: 30 March 2006  
Accepted: 19 April 2006  
© Springer-Verlag 2006

P. Mandare · H. H. Winter (✉)  
Department of Chemical Engineering,  
University of Massachusetts,  
Amherst, MA, USA  
e-mail: winter@ecs.umass.edu

**Abstract** Low shear rate and low frequency measurements focused on the extremely slow dynamics of a three-dimensional body-centered cubic (BCC) structure of an asymmetric block copolymer under nanophase-separated conditions. The material studied was poly(styrene-*b*-ethylene-*co*-butylene-*b*-styrene) swollen in a hydrocarbon oil selective for the midblock. Transient viscosities during start-up of shear flow at extremely low shear rates are governed by very long relaxation times and by a modulus that is nearly the same as the plateau modulus obtained from oscillatory shear experiments. Only at extremely low shear rates a zero shear viscosity could be attained. Its very high value is close to the

viscosity calculated from stress relaxation experiments. The steady shear viscosity decreases by several orders of magnitude when increasing the shear rate. SAXS experiments on samples sheared even at very low rates indicated loss of the BCC order that was present in the annealed samples before shearing. The SAXS profile recorded on such a sample showed a first-order maximum followed by a broad shoulder indicating a liquid-like short-range order of PS nanospheres in the swollen EB matrix.

**Keywords** Block copolymer · Slow dynamics · Steady shear viscosity · Dual structural model · Strain criterion · BCC order · Yield stress

### Introduction

Block copolymers nanophase-separate below a certain temperature, their “nanophase separation temperature”, the  $T_{NST}$ , and form ordered domains. The morphology of the ordered structure depends on temperature, volume fraction, and thermodynamic compatibility between the blocks. The equilibrium phase behavior of block copolymers is well understood [1]. For a polymer with two distinct blocks, in particular, when the composition of the two blocks is highly asymmetric, spherical domain morphology is obtained and the spheres of the minor block arrange on a body-centered cubic (BCC) lattice in a continuous matrix formed by the major block. The ordering of the nanospheres on a cubic lattice occurs only when cooling below a certain temperature that is called “lattice ordering temperature”,  $T_{LOT}$  [3, 8, 12]. This temperature is substantially

lower than the  $T_{NST}$ . At all temperatures between  $T_{LOT}$  and  $T_{NST}$ , the nanospheres of the block copolymer assume liquid-like short-range order (LSO) in the continuous matrix of the major phase [3, 7, 8, 12]. Additional temperature effects enter when the block copolymer is cooled below one of the nanophase-separated domains’ glass transition temperature, the  $T_g$ .

Rheology responds dramatically to small variations of order in nanophase-separated block copolymers. Hence, rheological measurements have become a valuable tool for characterizing structural changes in these materials. Studies of viscoelasticity mostly focused on classical phases of lamellae and hexagonally packed cylinders, often with the purpose of locating the transition temperatures. Less studied are the viscoelastic patterns and their analysis, especially for the cubic phases [2, 4, 9–11, 13, 17]. Watanabe and Kotaka [15, 16] and Hashimoto et al. [2]

---

performed steady shear rheology as well as small amplitude oscillatory shear on di- and triblock copolymers with cubic phases. However, the shear-rate range and the frequency range used in those studies were relatively narrow, and long-time behavior remained unexplored. A Bingham-type model, with modulus, viscosity, and yield stress as parameters, was found to express the stress as a function of shear rate. Kossuth et al. [4] were the first to address the viscoelastic behavior of di- and triblock copolymers with both gyroid and BCC phases in detail. They identified two distinct frequency regions in which the storage modulus plateaued. The plateau observed at high frequency was attributed to entanglements ( $G_N^0$ ) whereas the plateau observed at low frequencies and extending over several decades was attributed to the presence of the BCC lattice ( $G_{\text{cubic}}^0$ ). Kossuth et al. [4] also noticed that the magnitude of  $G_{\text{cubic}}^0$  is insensitive to the strain amplitude in oscillatory shear indicating a true linear response. The shapes of  $G'$  and  $G''$  at the lowest frequencies indicated liquid behavior. However, even in the study of Kossuth et al. [4], terminal behavior at low frequencies is not addressed. The long-time behavior can also be explored by steady shear rheology in a stress-controlled rheometer [9–11] where the cubic phase block copolymers exhibit very high zero shear viscosities at very low shear rates instead of a yield stress. To our knowledge, this was the first effort to explore very long-time behavior of these materials.

Very recently, Mandare et al. [5] studied long-time stress relaxation in a newly built device (“relaxometer”) that allows to quantitatively distinguish liquid flow from solid behavior and to measure extremely long relaxation times in transient stress relaxation experiments. Experiments on a nanophase-separated asymmetric block copolymer with BCC lattice (same sample as in this study) demonstrated that the linear relaxation modulus decays to zero over extremely long periods of time except at room temperature where the sample has an equilibrium modulus.

In this study, we are comparing the linear viscoelastic, long-time behavior with the behavior at very low shear rates. Classically, it has been observed that the complex viscosity  $\eta^*$  is well above the steady shear viscosity  $\eta$ . This is due to the fact that the complex viscosity is measured under conditions such that the structure in the material remains intact whereas the steady shear viscosity is measured under nonlinear conditions of deformation that causes the structure to dissolve. However, the rate of deformation is so low that the broken structure is able to reform while the flow continues. Thus, it is very interesting to compare the complex viscosity at low frequencies to the steady shear viscosity at corresponding low shear rates. If the structure in the material that is broken due to nonlinear deformations in steady shear flow can recover itself fast enough at low shear rates, the two viscosities should be comparable in value.

For exploring this phenomenon, we compare the dynamics at low shear rates to the relaxation at extremely

long times (stress relaxation experiment) and to the dynamic moduli at low frequencies. The goal of this study is to bring together the results from these different types of rheological experiments.

---

## Materials and methods

The poly[styrene-*b*-(ethylene-*co*-butylene)-*b*-styrene] triblock copolymer (SEBS; commercial name Kraton G1650) of this study contains about 29 wt% polystyrene and has a number average molecular weight  $M_n=94,000$  and a polydispersity index of 1.15. The midblock of the polymer was selectively swollen with an extender oil (commercial name Fina Vestan) having a number average molecular weight of about 600. All the samples used in this study contain 20 wt% of the triblock copolymer (termed as SEBS20 henceforth). The nanophase separation temperature is about 120 °C whereas the glass transition temperature of the polystyrene phase is about 60 °C [13]. From long-time stress relaxation experiments [5], we had concluded that SEBS20 behaves as liquid at elevated temperatures and has extremely long relaxation times.

---

## Sample preparation

The details of the sample preparation are discussed elsewhere [13]. Basically, a mechanical stirring device was used to dissolve the polymer in the oil at high temperatures (150–180 °C). The samples used in all of the rheological experiments were annealed at 100 °C for 2 h after a quench from 150 °C. Small angle X-ray scattering carried out after annealing confirmed the presence of BCC lattice in the sample. However, the sample was polycrystalline, i.e., the lattice directions were uniform within individual grains (about micron size) but varied randomly across the entire sample. The overall random orientation was confirmed by the concentric rings in the SAXS profiles. Very recently, Mortensen [6] studied shear-induced ordering in the same system by large amplitude oscillatory shear (LAOS). However, in this study, highly ordered structures were not obtained even after shearing at constant rate for longer times.

Uniformly, the initial structure for all the rheological experiments was BCC lattice with  $d_{110}$  spacing of about 28 nm and domain size of about 6 nm. It is emphasized that the sample had a polycrystalline nature (grains) exhibiting powder diffraction pattern. In the following, such sample with BCC lattice order will be called “BCC-SEBS20”.

---

## Rheological studies

Oscillatory and transient rheological studies were carried out in two types of instruments. A strain-controlled

instrument (ARES, TA Instruments) was used to measure linear oscillatory behavior and for transient experiments at constant shear rate. A stress-controlled instrument (Viscotech, ATS Rheosystems) was used to study creep at very low shear stress levels. Cone and plate fixtures of 25 mm diameter were chosen for all the experiments in both the instruments.

---

## Experimental techniques

The following four types of rheological tests were carried out on BCC-SEBS20 that was annealed at 100 °C before each experiment.

### Oscillatory strain sweeps

Dynamic strain sweeps were performed for studying the range of linear behavior at different shearing frequencies and different temperatures.

### Small amplitude oscillator shear (frequency sweeps)

Frequency sweeps were carried out on annealed BCC-SEBS20 at three different temperatures in a strain-controlled rheometer ARES (TA Instruments) using a strain amplitude of 0.04. Experiments at increasing strain amplitudes showed the extreme sensitivity of the BCC structure to strain. Frequency sweep data at different strain levels are compared with the corresponding results at  $\gamma_a=0.04$  from our previous paper [5].

### Transient and steady shear viscosity

Start-up of shear in ARES covered shear rates from  $2 \times 10^{-5}$  to  $10 \text{ s}^{-1}$ . To access even lower shear rates, the stress-controlled Viscotech was used. It was possible to maintain very low stress and measure the evolving strain with time. The slope of strain vs time gives the shear-rate value that was used to calculate the time-dependent viscosity. Experiments started at the lowest possible stress. Then the stress was increased in small steps and the procedure was repeated.

Start-up of shear at constant rate gives the evolution of viscosity and stress with time until a steady state is reached. From these, the start-up time can be estimated. The shear-rate-dependent viscosity can be fitted with empirical correlations such as power law, Carreau, Cross, Carreau-Yesuda, etc.

In general, either a zero shear viscosity exists at low shear rates or a yield stress dominates (with  $\eta \sim \dot{\gamma}^{-1}$ ). If a viscosity got established at very low shear rates, we could

determine a characteristic longest relaxation time from the onset of shear thinning.

### Stress relaxation after step strain

A small strain,  $\gamma_0$ , is applied to the material at time  $t=0$ , and the resulting stress  $\tau(t)$  is measured as a function of time. These define the relaxation modulus

$$G(t) = \frac{\tau(t)}{\gamma_0}$$

both for liquids and for solids as well. Here, we are especially interested in the “linear relaxation modulus” which is measured at a strain so small enough that it does not disturb the equilibrium structure of the sample. It is defined as

$$G^0(t) = \lim_{\gamma_0 \rightarrow 0} \frac{\tau(t)}{\gamma_0} .$$

The long-time limit of the linear relaxation modulus distinguishes liquid from solid behavior.

$$\lim_{t \rightarrow \infty} G^0(t) = \begin{cases} 0 \text{ (liquid)} \\ G_e \text{ (solid)} \end{cases}$$

Long-time stress relaxation data of the same material have been published earlier [5]. Details of the experiments and measurement technique and analysis are described there.

---

## Results

The BCC structure of annealed samples at 100 °C is extremely strain sensitive. This is shown through strain sweeps at different frequencies (Fig. 1). The linear viscoelastic range narrows as the shearing frequency is decreased. The terminal zone requires excessively low frequencies that are beyond the experimental range. Figure 2 shows data of storage and loss modulus against frequency for annealed SEBS20 at three different temperatures, viz., 25, 85, and 100 °C as measured in the preceding study [5]. The strain amplitude in these experiments was kept constant at 0.04. The sample exhibits two distinct plateaus in the storage modulus, one at higher frequencies with a value of about 20,000 Pa and second at low frequencies with a value of about 3,000 Pa. The plateau at low frequencies (observed at higher temperatures, 85 and 100 °C) extends over several decades in frequency. Although there is no low frequency crossover between  $G'$  and  $G''$ , even at a frequency of  $10^{-4} \text{ rad/s}$ , a minimum in  $G''$

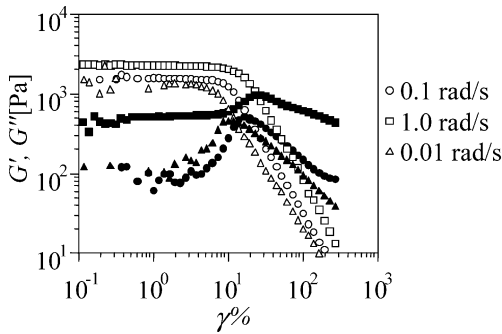


**Fig. 1** Strain sweep at 100 °C for SEBS20 annealed at 100 °C for different frequencies. *Open symbols* represent  $G'$  and *filled symbols* represent  $G''$

at intermediate frequencies suggests that such a crossover would occur at some very low frequency. As the strain amplitude is slightly increased, the minimum in  $G''$  moves to higher frequencies and, at even larger strain amplitudes, a crossover between the dynamic moduli is observed within the experimental frequency window (Fig. 3). In comparison, the magnitude of the low frequency plateau in  $G'$  is almost insensitive to strain amplitude. The shape of frequency sweep curves depends on the strain amplitude chosen, even at these very small amplitudes. The higher the strain amplitude, the higher is the frequency at which upturn in  $G''$  is observed and consequently the higher would be the crossover frequency. This indicates that the longest relaxation time depends on the strain amplitude chosen, and it remains unclear whether this is a true material response or a strain-induced effect.

To resolve this issue, we decided to measure steady viscosities at very low shear rates and see if we find a finite zero shear viscosity or a yield stress. Before starting each shear experiment, the sample was annealed at 100 °C for 2 h. A constant shear rate was applied (using ARES with cone and plate fixtures) until stress and viscosity had reached steady values. The shearing time required was proportional to the inverse of the shear rate used (Fig. 4). To more clearly show this phenomenon, we rescale the abscissa

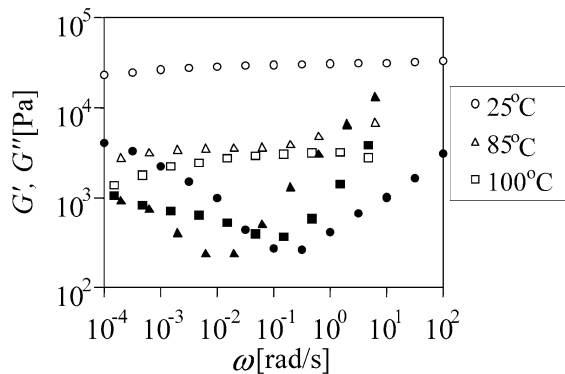


**Fig. 2** Storage and loss moduli of SEBS20 that was annealed at 100 °C. *Open symbols* represent  $G'$  and *filled symbols* represent  $G''$  [5]

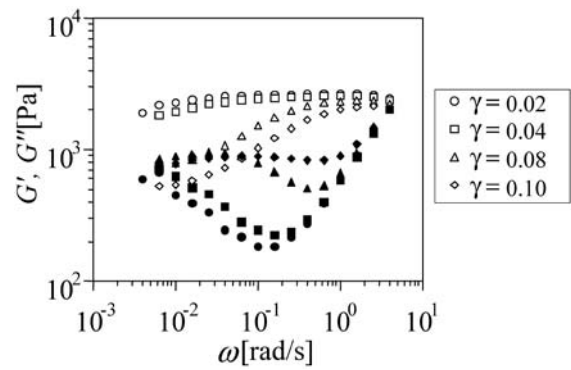


**Fig. 3** Storage and loss moduli of annealed SEBS20 at 100 °C at different strain levels. *Open symbols* represent  $G'$  and *filled symbols* represent  $G''$

and use the product of time and shear rate (Weissenberg number  $We$ ) which is a measure of nonlinearity in material behavior. In addition, the logarithmic time scale emphasizes the short-time behavior immediately after starting the flow. An overshoot in stress is observed at a strain of about 0.1. The magnitude of the overshoot increases with shear rate. The viscosity rises continuously at first. But then it peaks and reaches a steady value at a strain, which is approximately the same for different shear rates at least in the lower range of the shear rates.

The steady shear viscosity decays strongly with shear rate (Fig. 5). The lowest shear rate that could be accessed in ARES is  $2 \times 10^{-5} \text{ s}^{-1}$ . Even at such a low shear rate, a zero shear plateau was not attained. To investigate the variation of viscosity at even lower shear rates, we performed transient experiments in a stress-controlled rheometer, Viscotech, also using cone and plate fixtures. The linear growth of strain with time (Fig. 6) attests to the constant shear rate that establishes itself at a constant stress. From the slope, we determined the resulting steady shear rate and calculated the viscosity. The results from these two separate instruments (ARES and Viscotech) are plotted together in Fig. 7 as a function of shear rate. The inset in Fig. 7 shows the same data, however, with stress as abscissa. It can be seen that the material exhibits a zero shear viscosity plateau at extremely low shear rates (order of  $10^{-6} \text{ s}^{-1}$ ). The viscosity values are extremely high ( $10^7 \text{ Pa s}$ ). However, over a very narrow range of shear stress, the viscosity drops by 4 orders of magnitude. Sebastian et al. [9] first reported this type of behavior for a variety of chemically different block copolymers that formed cubic structures.

## Discussion

It might be argued that at these extremely low shear rates, the leveling off of the viscosity might be due to slip of the material at the surfaces of the rheometer fixtures. However, as will be shown below, the shear modulus during start-up in strain-controlled instrument is in accordance with the

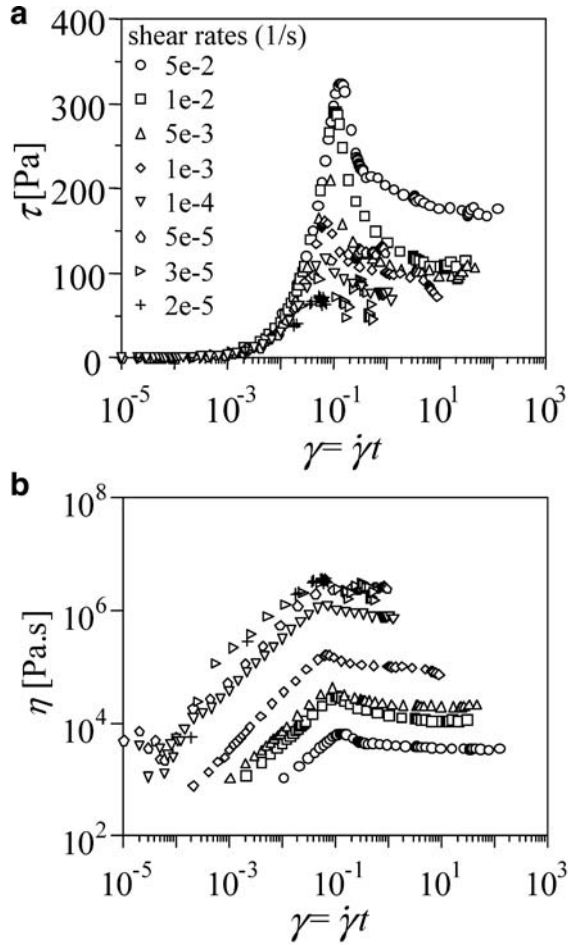


**Fig. 4** **a** Evolution of stress during start-up of shear on SEBS20 at 100 °C for different shear rates. **b** Evolution of viscosity during start-up of shear on SEBS20 at 100 °C for different shear rates (*same symbols* as in Fig. 4a)

modulus measured in oscillatory shear. Also, it will be shown that the observed steady viscosity is nearly equal to the viscosity obtained by separate experiments. This indicates that the observed high viscosities are indeed due to true response and not due to measurement artifacts.

The slope of viscosity vs shear-rate curve in Fig. 5 is about  $-0.9$ , which is close to the values reported in previous studies although those studies were carried out at much higher shear-rate values [2, 18]. This could have given rise to apparent solid behavior resulting in these materials being modeled by a Bingham-type equation with modulus and yield stress.

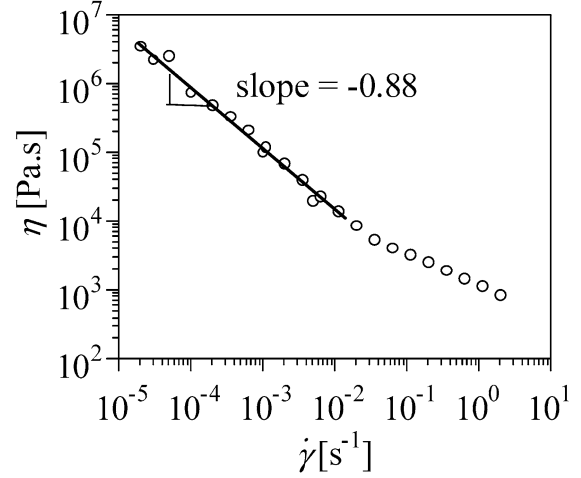


**Fig. 5** Viscosity as a function of shear rate for SEBS20 at 100 °C measured in strain-controlled instrument

The stress associated with a sudden drop in viscosity by several orders of magnitude (Fig. 7) may be viewed as a yield stress. The rate of strain below the critical stress is so low that the material appears to be a solid except when exposed to stress for extremely long times. A dual structural model [14, 20]

$$\eta(\dot{\gamma}) = \eta_I(\dot{\gamma}) + \eta_{II}(\dot{\gamma}) = \eta_{I,0} [1 + (\lambda_I \dot{\gamma})^{a_I}]^{(m_I-1)/a_I} + \eta_{II,0} [1 + (\lambda_{II} \dot{\gamma})^{a_{II}}]^{(m_{II}-1)/a_{II}}$$

with two vastly different relaxation mechanisms is able to describe such shear behavior phenomenologically. Both viscosities,  $\eta_I$  and  $\eta_{II}$ , are allowed to reduce with shear rate. However,  $\eta_I$  and  $\eta_{II}$  may shift differently with temperature because they represent different structures (at different length scales). Also, the finite recovery time of the structure is not explicitly involved in this steady-state viscosity model. The advantage of such constitutive model is its ease of use.

SEBS20 exhibits two distinct plateaus in  $G'$  reflecting two different relaxation mechanisms as discussed by Kossuth et al. [4]. The low frequency plateau is extremely sensitive to the strain amplitude as pointed out by the

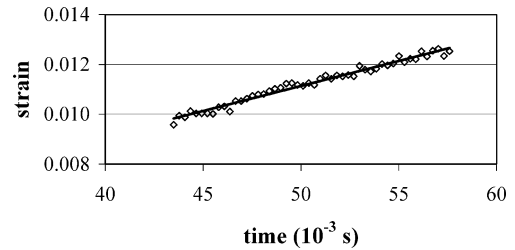
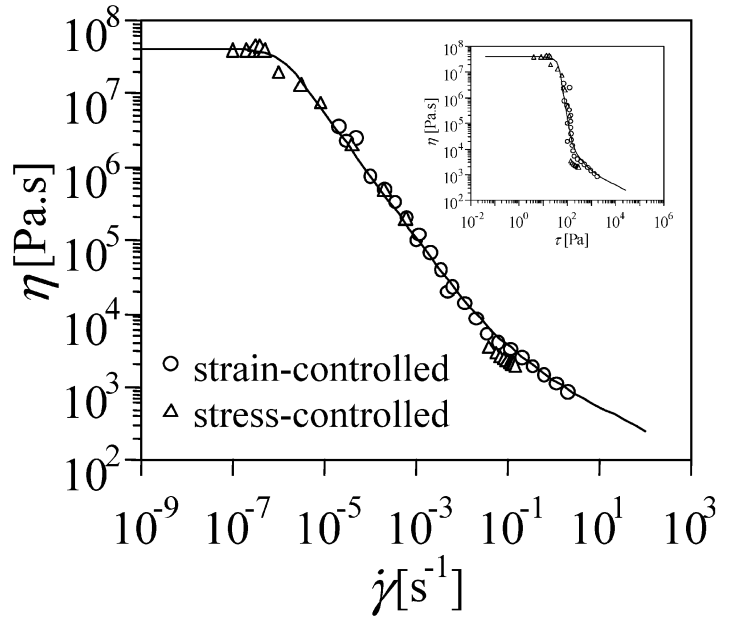


**Fig. 6** Evolution of strain in stress-controlled rheometer at prescribed shear stress = 8.0 Pa;  $T = 100$  °C; shear rate is given by the slope =  $2 \times 10^{-7} \text{ s}^{-1}$

**Fig. 7** Viscosity as a function of shear rate for SEBS20 at 100 °C showing zero shear viscosity (the *inset* shows same data as a function of shear stress). The *solid line* is obtained by fitting the data using dual structural model. The following parameter values were used for fitting:  $\eta_{I,0}=4.0e7$  Pa s,  $\lambda_I=1.0e6$  s,  $a_I=2.0$ ,  $n_I=0.14$ ,  $\eta_{II,0}=2.0e3$  Pa.s,  $\lambda_{II}=10.0$  s,  $a_{II}=2.0$ , and  $n_{II}=0.70$ . The parameters were calculated with the IRIS rheology platform program [19]



authors. The linear viscoelastic region is limited to extremely small strains. This has been addressed in the start-up experiments at very low shear rates.

Figure 8 shows stress and strain curves at low shear rates during start-up of shear. Replotting of data in Fig. 6 in a linear scale illustrates the behavior at short times more clearly. The initial slope of approximately 3,100 Pa is nearly the same as the plateau modulus at low frequencies obtained from the dynamic data. Linearity is observed only up to very small strain values (0.02–0.025). At large strain, shear thinning sets in and the stress passes through a maximum. Steady shear conditions are reached at a strain of about 0.06–0.07 at low shear rates. This, along with the observation of a modulus at early times, leads us to speculate that above this strain value, the BCC lattice in the sample breaks and the breaking gives rise to steady viscosity. We have carried out a few small angle X-ray experiments after shearing and quenching to room temperature (Mandare et al., manuscript under preparation). The X-rays show that the BCC lattice is destroyed by shear even though the exact shearing time (or strain) that is needed to break the lattice has not been determined yet. More work is being carried out to investigate this feature.

In the linear viscoelastic region, the viscosity is defined by the integral of the relaxation modulus. The viscosity data at 85 °C for SEBS20 was compared with our long-time stress relaxation data at same temperature measured in a totally different experiment [5]. Our previous work reported the data of relaxation modulus,  $G(t)$ , measured in

the “relaxometer”. The  $G(t)$  vs time data was fitted using a set of Maxwell modes ( $g_i, \lambda_i$ ), and the complex viscosity as  $\omega \rightarrow 0$  was calculated by

$$\eta_{\omega \rightarrow 0}^* = \sum g_i \lambda_i ,$$

where  $g_i$  is the relaxation mode and  $\lambda_i$  is the corresponding relaxation time. The viscosity value obtained from the stress relaxation experiments is  $7.6 \times 10^7$  Pa s whereas the constant shear-rate experiments yield a zero shear viscosity of about  $5.0 \times 10^7$  Pa s. It is surprising to find

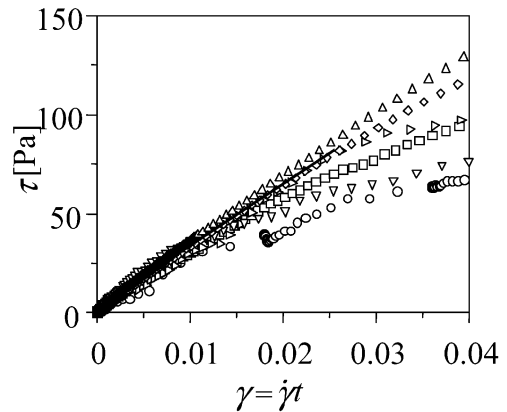


**Fig. 8** Stress during start-up of shear at 100 °C (same data as in Fig. 4a but plotted on linear scale up to only 4% strain). Slope in linear region is 3,100 Pa

that the viscosity measured in stress relaxation experiments (linear region) is only slightly higher than the viscosity measured in constant shear-rate experiments (nonlinear region). Even though the two values are not exactly the same, there is good agreement between the two values obtained from a set of totally different flow experiments in separate instruments.

The presence of such high zero shear viscosities and very long relaxation times was first reported by Sebastian et al. [9]. Using small angle X-ray scattering, these authors found that the BCC lattice remains intact during shearing at shear rates where a zero shear viscosity is observed. Thus, the existence of a zero shear viscosity was attributed to a different type of relaxation and not to the destruction of the BCC lattice. We also carried out small angle X-ray scattering experiments after shearing the sample at low stress levels that are governed by a zero shear viscosity. Figure 9 compares the SAXS profiles of an annealed sample and a sheared and quenched sample. The annealed sample clearly shows presence of primary and higher order peaks indicating a long-range order, whereas the profile of the sheared and quenched sample shows absence of higher order reflections indicating that the long-range order associated with the BCC lattice is lost due to shear even at very low shear rates. Instead, a broad shoulder is seen at  $q \approx 0.37 \text{ nm}^{-1}$ . This indicates that the structure obtained after shear consists of spheres of PS (indicated by a broad maximum due to form factor at  $q \approx 0.76 \text{ nm}^{-1}$ ), which assume LSO (primary peak at  $q \approx 0.021 \text{ nm}^{-1}$ ) as discussed in detail by Schwab and Stühn [8] and Kim et al. [3]. For asymmetric PS-PI diblock, Schwab and Stühn [8], using SAXS, demonstrated that there is a range of temperature below  $T_{\text{NST}}$  where the nanospheres assume LSO and exhibit similar broad shoulder and a form factor as seen in Fig. 9. For asymmetric SEBS without any solvent, Kim et al. [3], using SAXS, TEM, and rheology, demonstrated that there is a broad range of temperature in which spheres of PS assume LSO and subsequently dissolve above nanophase separation temperature to form a homogeneous

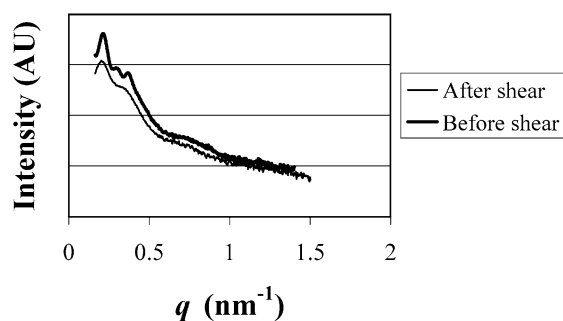


**Fig. 9** SAXS profiles recorded before and after the application of shear on SEBS20. The stress level during shear was 8 Pa

solution. In between lattice dissolution temperature and  $T_{\text{NST}}$ , their material also exhibited a shoulder after the primary peak similar to the one shown in Fig. 9. In this temperature range, the SAXS profile can be fitted using paracrystal theory. In this theory, the total scattering intensity is formulated using scattering from interparticle interference (structure factor) and intraparticle interference (form factor of spheres). This gives rise to a shoulder in the scattering profile when there is LSO in the material. From the similarity of the SAXS profiles obtained in this study and that of Schwab and Stühn [8] and Kim et al. [3], it seems that the structure of the sample obtained after shear and quench even at low rates is analogous to the one obtained after the dissolution of the BCC lattice. At ultralow shear rates, it is this LSO structure that is “shear-rate independent” exhibiting a constant but very high zero shear viscosity.

## Conclusions

All experiments were performed on nanophase-separated, annealed SEBS samples with polycrystalline (grains) BCC morphology. Small amplitude oscillatory shear experiments showed a plateau in  $G'$  at low frequencies. The magnitude of this plateau is insensitive to the strain amplitude in the linear viscoelastic range. However, the minimum in  $G''$  as well as the frequency at the crossover between  $G'$  and  $G''$  increases as the strain amplitude is increased, thereby making it difficult to measure a terminal relaxation time.

Steady shear rheology at extremely low shear rates ( $10^{-6} \text{ s}^{-1}$ ) is governed by an extremely high zero shear viscosity ( $10^7 \text{ Pa s}$ ). The modulus for stress growth during start-up of shear is nearly the same as the plateau modulus measured by oscillatory shear. Structure break-up seems to require a material characteristic strain. This is seen with the transient viscosity that requires about the same strain to reach steady state for all experiments at different rates of deformation. This strain is about equal to the strain amplitude for the onset of nonlinearity in oscillatory shear experiments.

The zero shear viscosity of steady shear flow is only slightly less than the viscosity obtained by integrating the relaxation modulus,  $G(t)$ , from a stress relaxation experiment. The relaxation times obtained from steady shear experiments (onset of shear thinning) are comparable to the ones previously measured in stress relaxation experiments [5]. The structure obtained through steady shearing, even at the lowest rates, corresponds to LSO of PS nanospheres in the EB matrix.

**Acknowledgement** This project is supported by the National Science Foundation (DMR-0213695) through the Materials Research Science and Engineering Center (MRSEC) at the University of Massachusetts Amherst.

---

## References

1. Bates FS, Fredrickson GH (1999) Block Copolymers—designer soft materials. *Phys Today* 52(2):32–38
2. Hashimoto T, Shibayama M, Kawai H, Watanabe H, Kotaka T (1983) Ordered structure in block polymers solutions. 2. Its effect on rheological behavior. *Macromolecules* 16:361–371
3. Kim JK, Lee HH, Sakurai S, Aida S, Masamoto J, Nomura S, Kitagawa Y, Suda Y (1999) Lattice disordering and domain dissolution transitions in polystyrene-block-poly(ethylene-co-but-1-ene)-block-polystyrene triblock copolymer having a highly asymmetric composition. *Macromolecules* 32:6707–6717
4. Kossuth MB, Morse DC, Bates FS (1999) Viscoelastic behavior of cubic phases in block copolymer melts. *J Rheol* 43(1):167–196
5. Mandare P, Horst R, Winter HH (2005) Long time stress relaxation of a triblock copolymer with asymmetric composition. *Rheol Acta* 45:33–41
6. Mortensen K (2004) Three-dimensional crystallographic determination of the body centered cubic morphologies of shear-aligned block copolymer systems. *J Polym Sci B* 42:3095–3101
7. Sakamoto N, Hashimoto T (1998) Ordering dynamics of cylindrical and spherical microdomains in polystyrene-block-polyisoprene-block-polystyrene. 1. SAXS and TEM observations for the grain formation. *Macromolecules* 31:8493–8502
8. Schwab M, Stühn B (1996) Thermotropic transition from a state of liquid order to a macrolattice in asymmetric diblock copolymers. *Phys Rev Lett* 76(6):924–927
9. Sebastian JM, Graessley WW, Register RA (2002a) Steady-shear rheology of block copolymer melts and concentrated solutions: defect-mediated flow at low stresses in body-centered-cubic systems. *J Rheol* 46:863–879
10. Sebastian JM, Lai C, Graessley WW, Register RA (2002b) Steady shear rheology of block copolymer melts: zero shear viscosity and shear disordering in body centered cubic systems. *Macromolecules* 35:2700–2706
11. Sebastian JM, Lai C, Graessley WW, Register RA (2002c) Steady shear rheology of block copolymer melts and concentrated solutions: disordering stress in body centered cubic systems. *Macromolecules* 35:2707–2713
12. Shibayama M, Hashimoto T, Kawai H (1983) Ordered structure in block polymer solutions. 1. Selective solvents. *Macromolecules* 16:16–28
13. Soenen H, Berghmans H, Winter HH, Overbergh N (1997) Ordering and structure formation in triblock copolymer solutions. Part I. Rheological observations. *Polymer* 22:5653–5660
14. Stephens T, Winter HH, Gottlieb M (1988) The steady shear viscosity of filled polymeric liquids described by linear superposition of two relaxation mechanisms. *Rheol Acta* 27:263–272
15. Watanabe H, Kotaka T (1982) Rheological and morphological diblock behavior of styrene–butadiene diblock copolymer solutions in selective solvents. *J Rheol* 26(2):153–179
16. Watanabe H, Kotaka T (1984) Rheology and structure of styrene–butadiene block copolymer melts dissolved in selective solvents. *Polym Eng Rev* 4:73–122
17. Watanabe H, Kuwahara S, Kotaka T (1984) Rheology of styrene–butadiene–styrene triblock copolymer in n-tetradecane systems. *J Rheol* 28(4):393–409
18. Watanabe H, Matsumiya Y, Kanaya T, Takahashi Y (2001) Rheology and structure of a butadiene–styrene diblock copolymer in dibutyl phthalate: role of concentration fluctuation in disruption and reformation of micellar lattice. *Macromolecules* 34:6742–6755
19. Winter HH, Mours M (2005) The cyber infrastructure initiative for rheology. *Rheol Acta* (in press). DOI 10.1007/s00397-005-0041
20. Winter HH, Stephens TS, Morrison F (1985) The dual structural model, a phenomenological constitutive equation for thixotropic fluids with yield. Annual meeting of Society of Rheology, Blacksburg, VA